Molecular Weight Effects and the Sequential Dynamic Nature of Poly(ethylene oxide) Adsorption on Silica from Polydisperse Aqueous Solution

V. A. Rebar and M. M. Santore*

Department of Chemical Engineering, Lehigh University, Bethlehem, Pennsylvania 18015

Received August 22, 1995; Revised Manuscript Received April 8, 1996[⊗]

ABSTRACT: Adsorption kinetics of a polydisperse sample of poly(ethylene oxide) were studied using total internal reflectance fluorescence (TIRF), a method whose signal is approximately proportional to the adsorbed chain *number*. The initial stages of the adsorption process were found to be approximately transport-limited, dominated by single-chain adsorption for free solution concentrations below 100 ppm and clusters at higher concentrations. In the intermediate stages of single-chain adsorption, an overshoot occurs. The timing of the overshoot is extremely sensitive to the molecular weight distribution of the sample, and various populations of different molecular weights within the sample can be resolved. The signal decrease after the overshoot is attributed to one or both of the following processes: replacement of initially adsorbed short chains with ones of higher molecular weight, or interfacial reconfigurations driven by the filling of the surface and affecting the quantum yield of the fluorescent tag on the chain end.

Introduction

Polymer adsorption is thought to involve three main steps: diffusion of chains to the interface, attachment, and interfacial reconfigurations. The first two steps are easily measured, but the nature of the third has been difficult to determine and is influenced by the exchange of chains between the layer and the free solution. Most studies of adsorption kinetics revealed the expected monotonic increase in surface excess toward equilibrium[1−7] (steps 1 and 2). Examples of early benchmark efforts in this area include ellipsometric studies of the adsorption of polystyrene (PS) onto chrome from toluene and carbon tetrachloride[2] and from flowing cyclohexane.[3] It was found that several hours was needed to achieve the equilibrium adsorbed amount: The layer thickness evolved first and the adsorbed layer densified over time.[2] Investigations of PEO adsorption on silica from deionized water using ellipsometry[4] and reflectometry[5,6] (including those in our laboratory[7]) revealed transport-limited adsorption. A radiotracer study of polyacrylamide adsorption onto modified glass from water found an increasingly slower rate of exchange of labeled and unlabeled chains as the layer aged.[8,9] Hence the approach to equilibrium was found, for some systems, to continue beyond the time scale of mass accumulation on the surface.

Several investigators, employing surface-sensitive techniques, found overshoots in the adsorption kinetics, possibly a result of surface reconfigurations (step 3). For example, overshoots in mass during the adsorption of styrene/ethylene oxide block copolymers from cyclopentane onto glass were detected by dynamic scanning angle reflectometry.[10] Total internal reflection fluorescence (TIRF) studies of fluorescein isothiocyanate (FITC)-tagged poly(dimethyldiallylammonium-*co*-acrylic acid) adsorbing on quartz from aqueous buffer revealed fluorescence overshoots that intensified with increasing polymer concentration.[11] During the adsorption of diblock and triblock copolymers of PEO/PS from toluene on silica, overshoots were detected using null ellipsometry.[12] In TIRF studies, eosin-labeled RNase adsorbing from aqueous buffer onto PS exhibited a fluorescence overshoot.[13] FTIR-ATR revealed overshoots in adsorbed mass during poly(dimethylsiloxane) and *cis*-polyisoprene adsorption from carbon tetrachloride on silica or germanium.[14] These overshoots were attributed to surface micelle relaxations,[10] reconfigurations driven by chemical heterogeneity in polymers[11,12] and proteins,[13] and surface crystallization.[14]

The current findings provoke further studies of polymer adsorption kinetics, especially the role of slow interfacial relaxations (nonequilibrated layers), and the occurrence of interfacial reconfigurations which reflect surface loading (possible at local equilibrium). TIRF provides a means to closely follow such processes over the course of days, because the experiments can be run in modes sensitive to factors other than surface mass, and the signal is generally more stable than refractive index based methods.

This paper explores overshoots in fluorescence signal during the adsorption of FITC-labeled PEO (FPEO) onto silica from aqueous solutions.[15−17] Such overshoots were also found for rhodamine-tagged PEO. This overshoot is greatly influenced by the molecular weight distribution of the sample and may reflect interfacial reconfigurations or exchange between various populations within the sample.

The previous paper,[17] which employed TIRF to probe static (or apparent equilibrium) aspects of adsorption, raised several issues concerning history-dependent adsorption behavior and the accuracy of internal TIRF calibrations. For FPEO it was found that the adsorption isotherms measured via TIRF were the same shape as those measured on silica particles, as long as sufficient equilibration time was provided in the TIRF cell. The internal TIRF calibrations, however, revealed a lower quantum yield by a factor of ∼5 for fluorophores on adsorbed chains compared with those in free solution, indicating that quenching and adsorption processes occurred simultaneously. It then becomes an issue for adsorption kinetics studies whether the TIRF signal is proportional to the surface fluorophore concentration over the full course of the adsorption process. Signal linearity would be expected, and valuable kinetic information obtained, in experiments where all adsorbed

[⊗] Abstract published in *Advance ACS Abstracts,* August 15, 1996.

S0024-9297(95)01237-X CCC: $12.00

chains were quenched to the same extent and where the same time scale intrinsic to the interfacial quenching processes was more rapid than that of adsorption or chain arrival to the surface.

The issue of signal linearity is addressed here from a kinetic perspective. Findings argue in favor of linearity in the early and late stages of the adsorption process, and several possibilities are presented for intermediate times. A concept central to the arguments presented here is that polydisperse samples containing end-tagged chains yield TIRF signals proportional to interfacial chain number. The previous paper explored how this labeling topology can affect the quantitative determination of the surface coverage, and in this work we show that kinetic traces based on chain number may differ drastically from those based on chain mass, for example ellipsometry and reflectivity. Because of the end-labeling topology, it is reasonable to expect overshoots in the TIRF signal as the molecular weight distribution on the surface evolves during the course of the adsorption process. The current work explores the extent to which the overshoot can be attributed to exchange between high and low molecular weight populations within polydisperse end-tagged samples, when high molecular weight chains are preferred, ultimately on the surface. Overshoots were not found for randomly tagged (hydroxyethyl)cellulose (HEC)[17] or with FPEO adsorption on polystyrene films.[18,19] In the former case, the TIRF signal is proportional only to surface mass while in the latter case, there is evidence that fluorescein−surface attractions diminish the molecular weight selectivity of the adsorption process.

Experimental Section

Materials. Several molecular weights of PEO were used in this investigation. Monodisperse 97K PEO was purchased from Polymer Laboratories, polydisperse 100K and 400K PEO were obtained from Aldrich, and monodisperse 20K PEO was purchased from Polysciences, Inc. The fluorescent label was fluorescein isothiocyanate (FITC) isomer I from Sigma. FITC was covalently attached to the hydroxyl groups on the 97K chain ends, and samples were purified by dialysis as previously described.[17−20] The maximum labeling density was 1 tag/chain because these PEO chains originally had hydroxyl groups on only one of two ends. During storage in deionized (DI) water, degradation of the labeled 97K sampled (denoted FPEO) gradually occurred via a free radical mechanism, and the molecular weight distribution was periodically checked with gel permeation chromatography (GPC). At the time of this study, the polydispersity had increased, the distribution appeared bimodal, and the average molecular weight was close to 65K. It is unclear if the apparent bimodal nature of the sample was real or due to the influence of the label on the retention time of the low molecular weight chains.[20] The 20K, 100K, and 400K samples were not labeled, but subject to the same dialysis procedure as the FPEO, and stored in DI water prior to use.

Acid-washed microscope slides (soda lime glass, Erie Scientific) served as planar silica surfaces for TIRF adsorption experiments. The slides were soaked in concentrated sulfuric acid for at least 10 h in the flow cell assembly prior to each run. Before starting a run, the acid was removed by thoroughly flushing the cell with DI water to yield a silica surface.[21] One micron diameter spherical silica particles (Geltech) provided a dispersed silica surface for adsorption isotherm screening studies. XPS studies of the two silica surfaces revealed nearly identical surface compositions, making it reasonable to expect similar adsorption behavior on particles and slides.[20]

Polymer adsorption was conducted in phosphate-buffered saline (PBS, containing 147 mM NaCl, 2 mM KH_2PO_4, and 8 mM Na_2HPO_4) which maintained the solution pH near 7.4. This was necessary because fluorescein is very pH sensitive near pH 6, that of DI water.[21,22] PBS regulates the ionic environment at the silica surface, maintaining strong fluorescence from adsorbed FPEO during adsorption studies.[21]

The fluorescence of the polymer solutions was measured with a Turner filter fluorometer to generate calibration curves for adsorption isotherm studies. It contained a mercury lamp with a broad blue gel filter excitation near 475 nm, and the fluorescence was monitored above 540 nm through a sharp-cut high-pass filter (Schott SOG530). Based on a comparison of the fluorescence of FPEO in PBS to FITC solutions of known concentration, the labeling of this sample was approximately 60% complete.

Methods. The interpretation of the TIRF results was aided by a comparison with a second method for measuring polymer adsorption: mass balance type adsorption isotherms using spherical silica particles. Isotherms were measured for the FPEO sample and for mixtures of FPEO and unlabeled PEO. Each isotherm employed a separate calibration curve (fluorescence vs polymer concentration), based on the total PEO content in the sample of interest. Isotherm data were obtained by mixing 0.5 g of dry silica particles with 7.0 g of FPEO or mixtures containing 20 wt % FPEO with the balance unlabeled PEO. The solution−particle mixture was shaken by hand for 15 min and then allowed to equilibrate for 12−24 h, during which time the particles settled by gravity. The fluorescence of the supernatant was measured and the free concentration of FPEO or the FPEO/unlabeled PEO mixture was determined from the appropriate calibration curve. The adsorbed amount was calculated from a mass balance. The use of calibration curves in this fashion directly tracked the changes in the concentration of labeled chains and allowed us to determine whether there was any selective partitioning of labeled and unlabeled populations between the free solution and the surface. Selectivity for or against labeled populations would alter the fluorescence per unit mass in the free solution and on the surface and, through the use of calibration curves, introduce error if the adsorption data were reported on a total mass basis.

Total internal reflectance fluorescence (TIRF) was used to measure adsorption kinetics in a flow cell with an adjustable wall shear rate. The details of this method[23−25] and our apparatus in particular[17,19−21] have been summarized elsewhere. In these studies, we employed a penetration depth of 65 nm, laser excitation at 488 nm, and photon counting detection above 540 nm. Black flow cells[17,19] were employed to minimize the scattered light contribution to the signal, and flow was maintained by a syringe pump.

Convection Diffusion Model. In this study, a convection diffusion model provided two types of information: An analytical expression for the dependence of the transport-limited adsorption on experimental parameters (per the solution of Leveque[26]), and a means of independently measuring an average diffusion coefficient of the adsorbing species. Both modeling efforts begin with the convection diffusion equation for a slit geometry, previously presented[24,25] and given here in dimensionless form:

$$\frac{\partial C}{\partial \tau} + \eta(1 - \eta Pe^{-1/3})\frac{\partial C}{\partial X} = \frac{\partial^2 C}{\partial \eta^2} \tag{1}$$

Here C is the dimensionless concentration of the diffusing species normalized on that of the bulk solution, and τ is dimensionless time. X is the dimensionless flow direction, parallel to the substrate and normalized on the distance from the entrance port to the point of observation, $L_\infty = 2.5$ cm. η is the dimensionless distance from the substrate into the solution normalized on the diffusive boundary layer thickness:

$$\eta \equiv Pe^{1/3} y/H_\infty \tag{2a}$$

$$Pe \equiv \frac{\gamma H_\infty^{\,3}}{D L_\infty} \tag{2b}$$

y is the actual distance perpendicular to the substrate, H_∞ is the cell depth, in our case 0.4 or 0.5 mm, and the Peclet number, Pe, includes the wall shear rate γ and the diffusion coefficient D. The dimensionless time, τ, is defined

$$\tau = \frac{t}{L_\infty Pe^{1/3}/(\gamma H_\infty)} \tag{3}$$

where t is the actual time. Initially, the cell contains flowing solvent, but after a valve turnover at $\tau = 0$, a polymer solution progresses through the cell in the X direction. This gives the initial condition:

$$C(\tau{=}0) = 0 \qquad \text{for } X > 0 \text{ and } \forall\ \eta \tag{4a}$$

$$C(X{=}0,\tau{=}0) = 1 \qquad \text{for } \forall\ \eta \tag{4b}$$

and the boundary condition far from the surface:

$$C(\eta{\rightarrow}\infty) = 0 \qquad \text{for } \tau < \tau_c \tag{5a}$$

$$C(\eta{\rightarrow}1) = 0 \qquad \text{for } \tau \geq \tau_c \tag{5b}$$

with contact time, τ_c, defined

$$\tau_c = \frac{X}{\eta(1 - \eta Pe^{-1/3})} \tag{5c}$$

Following Shibata and Lenhoff,[25] we found it adequate to apply the condition in eq 5 at $\eta = 4$.[27,28]

For transport-limited adsorption, fast chain attachment on the surface depletes the nearby solution of polymer. The Leveque approximation[26] for a pseudo-steady-state solution to eq 1 also includes a fixed concentration gradient near the surface and omits the time dependence in eq 1:

$$\frac{dC_s}{dt} = \frac{1}{\Gamma(4/3)9^{1/3}}\left(\frac{\gamma}{DL_\infty}\right)^{1/3} DC_0 \tag{6}$$

Here, dC_s/dt is the rate of chain arrival from the bulk to the surface, which is proportional to C_0, the bulk polymer concentration, the wall shear rate to the one-third power, and the diffusion coefficient to the two-thirds power. The one-third power law for the adsorption rate is an important result we later exploit.

The application of eq 6 to the experimental data requires an accurate value of the single-chain diffusion coefficient, D. The convection diffusion model provides an independent means of extracting D from experiments where (through treatment of the surface) FPEO adsorption is prevented. In this case, the boundary condition for nonadsorbing diffusers is

$$\left.\frac{\partial C}{\partial \eta}\right|_{\eta\rightarrow 0} = 0 \qquad \forall\ \tau \tag{7}$$

Equations 1−5 and 7 were solved numerically[27] to determine the evolution of the free concentration at the point of observation, $C(\eta{=}0,X{=}1)$, as a function of τ for different values of the Pe. We employed the program of Kelly, which incorporated the evanescent penetration depth to predict the fluorescence evolution in a zone near the surface.[27] The best fit of this model to the data led to an evaluation of D, an average which represents the fluorescently labeled species in the solution. The Stokes−Einstein equation,

$$D = \frac{kT}{6\pi\mu R_H} \tag{8}$$

was then used to calculate the average hydrodynamic radius, R_H, of the diffusing species. Here k_B is the Boltzmann constant, T is the absolute temperature, and μ is the viscosity of water. In our determination of D, the surface was rendered nonadsorbing by a preadsorbed layer of FPEO.

Results

1. Effect of Molecular Weight on Coverage. Typically, adsorption isotherms report the total adsorbed amount of polymer vs the total concentration of polymer in the bulk solution at equilibrium. Figure 1a presents an alternate way of viewing adsorption data,

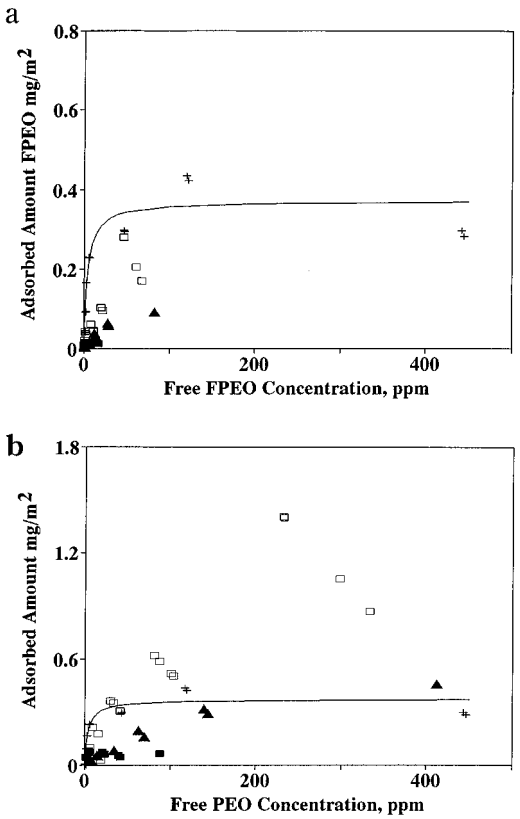

Figure 1. Adsorption isotherms on 1 μm silica particles for FPEO (+) and for mixtures containing 20 wt % FPEO and 80 wt % of the following: unlabeled 20K PEO (□); unlabeled 100K PEO (■); unlabeled 400K PEO (▲). (a) Adsorbed amount of FPEO vs concentration of FPEO in bulk solution; (b) Apparent total adsorbed amount of PEO vs total concentration of PEO in bulk solution.

which compares the adsorption isotherm of FPEO alone to FPEO adsorption in the presence of unlabeled chains of different molecular weights. Only the concentration of FPEO, both on the surface (ordinate) and remaining in solution (abscissa), is shown for the mixture experiments. Unlabeled chains may, however, be present in free solution and on the surface. A Langmuir-type curve is drawn though the data for the control FPEO sample (no PEO present) only to guide the eye. No physical significance is attributed to this curve form. The remaining points represent adsorption results from mixtures containing a total of 20 wt % FPEO and 80 wt % unlabeled PEO of molecular weight 20K, 100K, or 400K. The mixture experiments span the same range of total polymer concentrations as the experiments with the pure FPEO sample.

The FPEO isotherm shape is typical of high-affinity adsorption, with a steep initial rise and a distinct plateau near 0.4 mg/m^2. In the mixtures, the adsorbed amount of FPEO is reduced because unlabeled chains now compete with the labeled ones for the surface. Furthermore, higher molecular weight PEO (100K and 400K) is more effective than lower molecular weight PEO (20K) in reducing FPEO adsorption. The fact that unlabeled 20K chains reduce FPEO coverage means that the FPEO sample must contain some labeled populations with molecular weights below 20K and that the unlabeled 20K PEO chains are preferred on the surface rather than the low molecular weight populations within the FPEO sample.

Figure 1a suggests that high molecular weight chains are more effective in preventing FPEO adsorption than other factors, such as the potential effect of the FITC

tag. Because the representation in Figure 1a does not take into account free chains, additional insight is gained when the same data are plotted in the conventional isotherm form of total adsorbed amount of polymer vs total free polymer concentration, shown in Figure 1b. Here the free polymer concentrations were determined from calibration curves for total polymer vs fluorescence, and the adsorbed amounts calculated via a mass balance. Obtaining the free polymer concentration in this manner does not distinguish between labeled and unlabeled chains and presumes no surface preference for labeled or unlabeled chains. Without surface selectivity for a particular population, the mixture data, when represented as in Figure 1b, would be identical to the control experiment with the original FPEO sample. The differences between the control FPEO isotherm and those for the mixtures, then, provide a measure of the extent to which the surface is selective for different molecular weight populations.

In Figure 1b, a Langmuir-shaped curve is drawn through the points for the FPEO sample to guide the eye. For the mixtures containing unlabeled PEO chains with molecular weights (100K and 400K) exceeding the original FPEO sample, the data lie below the control isotherm, demonstrating that the higher molecular weight unlabeled chains are preferred on the surface. For the mixture which contained a total of 80% unlabeled 20K chains, a good deal of the data show coverages which exceed the control isotherm. This observation demonstrates that at high free polymer concentrations, a component of the labeled FPEO sample is preferred on the surface over the unlabeled 20K chains. When labeled populations adsorb preferentially from a mixture, the supernatant phase becomes rich in free unlabeled chains such that the use of the original calibration curve (for total polymer) to gauge the free polymer concentration artificially elevates the apparent coverage. Therefore, a comparison of Figures 1a and 1b suggests that the labeled FPEO sample is mostly lower in molecular weight than the 100K and 400K samples of unlabeled PEO. Also, some fraction of the FPEO sample was lower in molecular weight than the narrow 20K sample, while a significant portion of the FPEO sample was greater than 20K in molecular weight. The overall trends suggest that the molecular weight of the labeled populations, not the chemical nature of the labels themselves, is responsible for the surface selectivity. Indeed, the surface selectivity for high molecular weight chains is an established feature of homopolymer adsorption.[1]

The selectivity of the silica for high molecular weights was also probed by using GPC to examine the molecular weight distribution of an FPEO solution before and after contact with silica particles. (The solution concentration prior to particle contact was 100 ppm and afterward it was 47 ppm, based on the calibration curve.) Figure 2 shows that the molecular weight distribution of the original FPEO sample (curve a) was very broad and appears bimodal, while after particle contact the distribution (curve b) was considerably narrower and of lower molecular weight. (In this figure, the *x* axis is given as retention time, instead of being converted to molecular weight: Though the columns could resolve the molecular weight distribution, there was considerable error in assigning a particular retention time an exact molecular weight.) The GPC results therefore support the explanation of surface selectivity for high molecular weight chains.

2. Adsorption Kinetics. Figure 3 illustrates four adsorption kinetic traces, each beginning with the adsorption of FPEO from 2 ppm solutions flowing through the TIRF cell at a wall shear rate of 8 s^{-1}. Run a, also shown in the inset, proceeds uninterrupted: Adsorption begins at time zero, a few minutes after a valve turnover that replaces flowing DI water with an FPEO solution. Early adsorption appears as a near-linear fluorescence rise to a sharp maximum. The signal then decays over the next several hours. Typical runs lasted up to 6 h, at which time the signal was still slowly decaying.

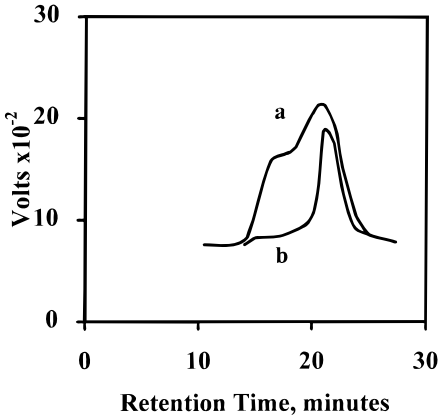

Figure 2. GPC results for (a) FPEO prior to contact with silica particles and (b) after contact of an initially 100 ppm solution with silica particles.

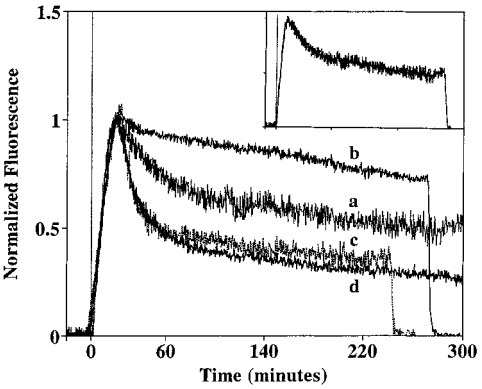

Figure 3. Adsorption of 2 ppm solutions at 8 s^{-1} wall shear rate: (a) FPEO; (b) FPEO with PBS switch at the maximum; (c) FPEO with switch to unlabeled 100K PEO at the maximum; (d) FPEO with switch to unlabeled 20K at the maximum. The inset shows the adsorption of (a).

To determine the cause of the overshoot, and more precisely, the processes involved in the decay, Figure 3 compares continuous run a with runs b–d in which the flow channel contents are switched near the anticipated maximum, but the same wall shear rate maintained. In run b, the FPEO solution was changed, after 23 min of flow, to PBS, a procedure which results in a decay that was more gradual than that of the uninterrupted run. In runs c and d, 2 ppm solutions of unlabeled 100K and 20K PEO, respectively, were introduced after 23–25 min of FPEO flow. In these runs, the fluorescence decay was similar in time scale but more extensive than that of the uninterrupted FPEO run in curve a. It is apparent from Figure 3 that labeled or unlabeled free chains drive a significant signal decrease in the middle and late stages of an adsorption experiment and cause the overshoot adsorption kinetics. That unlabeled chains are more effective in this regard negates the possibility that fluorophore–fluorophore interactions, which quench the fluorescence, result from continued addition of fluorophores to the surface.

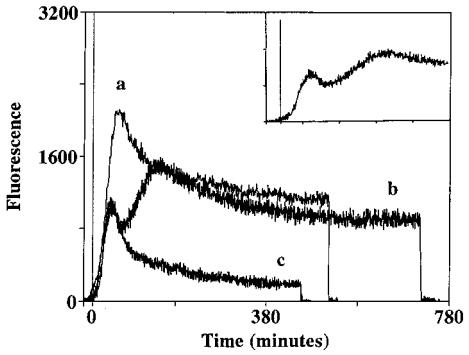

Figure 4. Adsorption of 2 ppm solutions at 0.8 s^{-1} wall shear rate in the TIRF apparatus: (a) FPEO; (b) 50/50 mixture of FPEO and unlabeled 20K PEO; (c) 50/50 mixture FPEO and unlabeled 400K PEO. The inset shows the initial adsorption details of (b) more clearly.

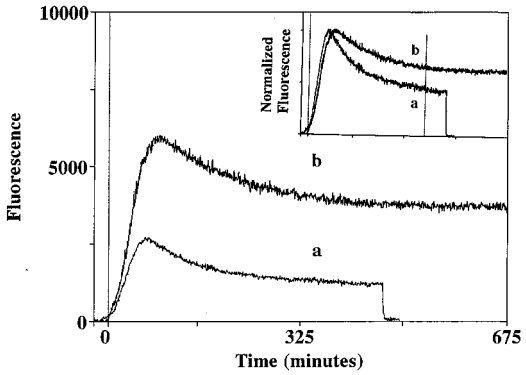

Figure 5. Adsorption of FPEO solutions at 0.8 s^{-1} wall shear rate in the TIRF apparatus: (a) 2 ppm FPEO; (b) FPEO diluted from apparently 47 ppm supernatant remaining after initial 100 ppm contact with silica particles to 2 ppm. The inset shows the data after normalization on the maximum fluorescence of each run; the line indicates 350 min of polymer solution flow.

TIRF adsorption experiments employing mixtures of the FPEO sample with unlabeled PEO illustrated the dramatic effect of molecular weight distribution on the shape of the overshoot. Figure 4 shows these experiments, conducted at a total polymer concentration of 2 ppm and at a wall shear rate of 0.8 s^{-1}, conditions which produced a slow rate of chain arrival to the surface so that all the kinetic features could be resolved. The curve labeled (a) is an uninterrupted run with FPEO, like that in Figure 3, but here at a wall shear rate of 0.8 s^{-1} rather than 8 s^{-1}. Curves b and c represent 50−50 wt % mixtures of FPEO with 20K and 400K unlabeled PEO, respectively, with a total concentration of 2 ppm. Also tested, but not shown, was a 50−50 wt % mixture of FPEO and unlabeled 100K PEO, whose adsorption trace closely resembled curve c for the mixture containing unlabeled 400K PEO. The ordinate in Figure 4 shows the raw fluorescence signal and is not normalized, as all three runs should not necessarily achieve the same maximum fluorescence or for that matter share the same initial slope. Indeed, the maximum fluorescence for the 400K PEO containing mixture is approximately half that for the FPEO run in curve a and its decay more rapidly approaches a smaller fraction of the maximum. For run b with the mixture containing unlabeled 20K PEO, two overshoots were observed and the ultimate signal level approached that of the FPEO run in curve a. We feel it may have been coincidental that the first overshoot of run b neatly collapsed onto the single overshoot of run c. The inset in Figure 4 shows the initial section of curve b to facilitate a clear view of the double overshoot.

One hypothesis to explain the overshoot adsorption kinetics is that the molecular weight selectivity of the surface drives the signal down at long times: The higher molecular weight chains ultimately dominate the surface and displace short early-arriving chains. Because of the fluorescein attachment on the ends of the original chains, the longer chains contain fewer fluorophores per unit area of adsorbed mass, giving rise to the unconventional kinetic traces. Such a hypothesis motivates studies with FPEO samples of narrow molecular weight distribution. These were not available, due to the degradation associated with the purification and wet storage of labeled PEO; however, a method was devised for obtaining a narrower fraction of the original sample. This was accomplished by diluting to 2 ppm the supernatant (apparently 47 ppm) that remained after the contact of an initially 100 ppm FPEO solution with silica particles. The GPC results for the narrow cut compared with the initial FPEO were presented in Figure 2. The narrower sample had fewer, if any, high molecular weight chains. Since this sample was lower in average molecular weight than the original sample, it contained a greater number of fluorophores per unit mass. Therefore, the use of the original calibration curve to determine an equivalent concentration of 47 ppm (prior to dilution) quite likely overestimated the actual concentration of polymer by as much as a factor of 2−5. Although after dilution the fluorescence of the narrower fraction matched that of a 2 ppm solution of the original sample, demonstrating equal concentrations of fluorophores, the mass concentration and average molecular weight of the narrow fraction were lower.

Figure 5 compares the TIRF-measured adsorption kinetics of 2 ppm solutions of the FPEO control, curve a, and the narrower molecular weight FPEO fraction of the sample, curve b. Several large differences between the two curves are evident. The first is that the fluorescence signal of the narrower sample (curve b) is about twice that of the original's (curve a). This occurs because the fluorescence per unit mass of the narrower sample is greater, leading to more fluorophores on the surface for a similar adsorbed mass. A comparison of the time corresponding to the maximum fluorescence reveals that the duration of the signal rise for the narrower fraction is nearly 50% longer than that for the FPEO. The extent of the overshoot decay within the time of these experiments is less for the narrower molecular weight fraction compared with the unfractionated FPEO control. The inset in Figure 5 more clearly illustrates this observation; here the vertical line denotes 350 min of polymer solution contact with the surface. The ratio of the fluorescence at 350 min to that at the maximum is 0.49 for the original FPEO sample and 0.68 for the narrower, lower molecular weight fraction.

3. Effects of Wall Shear Rate and Concentration. Adsorption studies were conducted at several wall shear rates to determine how closely FPEO adsorption kinetics approached the transport-limited extreme. The wall shear rate was found to affect both the initial rates of fluorescence increase and overshoot decay. In the late stages of these adsorption experiments (several hours after the initial FPEO contact), the effect of the wall shear rate on the overshoot decay diminished. Figure 6 illustrates these findings for 2 ppm FPEO solutions adsorbed at wall shear rates of 0.8, 8, and 80 s^{-1}. Here data are normalized on the maximum fluorescence level to reduce the impact of day-to-day baseline variations. Implicit in the normalization is that the wall shear rate

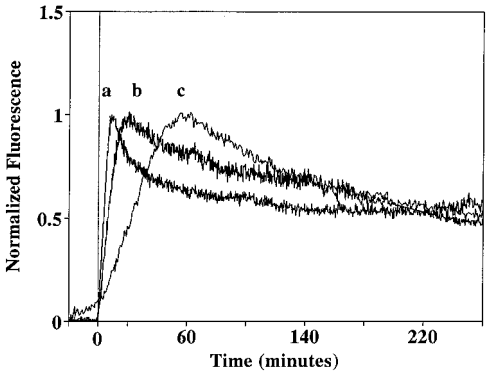

Figure 6. Adsorption of 2 ppm solutions of FPEO at various wall shear rates: (a) 80, (b) 8, and (c) 0.8 s^{-1}.

does not perturb the configurations of the absorbing chains or those in the layer, a reasonable assumption for wall shear rates in the range of 0.8−80 s^{-1} and molecular weights near 100K. A second issue is whether competition between the time scales for chain arrival and surface relaxations impart a wall shear rate dependence to the evolution of the surface coverage. If this were the case, a normalization such as that in Figure 6 would be inappropriate. Because we saw no trend in the maximum signal level with wall shear rate, it appears that the relaxation issue does not come into play at the point. In Figure 6, the lowest rates of fluorescence rise and fall occurred at the lowest wall shear rates, suggesting that incoming chains drive the signal up, then down, and that diffusion from the bulk solution is influential over a significant period of the adsorption experiments.

All the data up to this point have involved bulk polymer solutions sufficiently dilute such that the TIRF method was sensitive only to fluorophores within the adsorbed layer. At high bulk concentrations, the contributions of the free and adsorbed chains to the signal may evolve on separate or competing time scales. In studies targeting the effects of concentration on the overshoot shape, the concentration range includes conditions where the TIRF signal is influenced by fluorophores on free chains in the evanescent zone near the surface and, through scattered light, those in the main flow channel. The bulk signal evolution from the former reflects the diffusion of free chains from the main flow channel to regions near the surface, while that from the latter reflects the progression of the labeled polymer through the flow chamber.

Parts a and b of Figure 7 demonstrate the impact of the free FPEO concentration on the adsorption kinetics. In Figure 7a, dilute solutions of FPEO having concentrations of 2, 10, 20, 35, and 50 ppm are introduced in increasing order of concentration, while in Figure 7b the concentration sequence is 50, 100, 200, and 6255 ppm. Each polymer solution contacts the surface for 45 min followed by 45 min of flowing PBS, at a wall shear rate of 8 s^{-1}. Over the course of these runs, especially in Figure 7a, an underlying decay is apparent; however, in the short time periods when PBS is introduced just after a FPEO solution of moderate or high concentration, a rapid signal drop occurs due to the removal of free FPEO chains from the flow cell. This bulk signal contribution is approximately proportional to the bulk concentration and is distinct from the signal from adsorbed chains. Indeed for FPEO concentrations of 2 and 10 ppm, the free-chain contribution to the TIRF signal is within the experimental noise.

In Figure 7a, which involves concentrations near the shoulder of the FPEO isotherm in Figure 1, the most

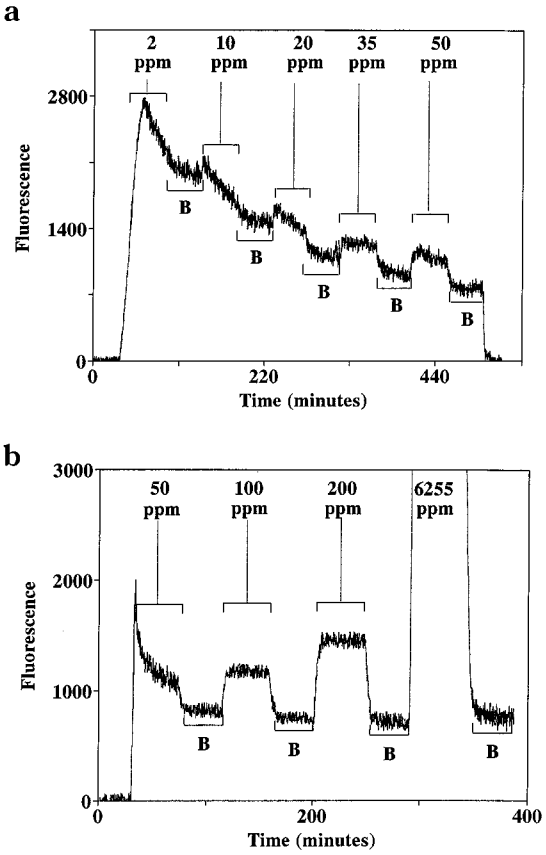

Figure 7. Sequential adsorption of FPEO solutions in order of increasing concentration at 8 s^{-1} wall shear rate with PBS washing (B) in between each polymer solution: (a) FPEO concentrations from 2 to 50 ppm; (b) FPEO concentrations from 50 to 6255 ppm.

dilute solution produced the largest fluorescence overshoot, with the magnitude of the overshoot decreasing with successive injections. The coverage at the time of the injection of each new solution was presumably greater than that at the time of injection of the previous solution. In Figure 7b, which focuses on concentrations on the plateau of the isotherm, the overshoot occurs only for the solution where the adsorption is most likely, adsorption of 50 ppm FPEO on a bare surface. For concentrations exceeding 100 ppm, the adsorption isotherm plateau has been reached and the surface has been saturated prior to the injection. Comparison of parts a and b of Figure 7 demonstrates that the overshoots occur in instances where addition of chains to the surface is most likely: on the rising part of the isotherm, during an adsorption history where the surface is not yet saturated, or for any concentration contacting an initially bare surface.

Separate experiments for the effect of free FPEO concentration on the adsorption kinetics on a bare surface at a wall shear rate of 13 s^{-1} are shown in Figure 8. The initial rates of signal rise and decrease are slowest at the lowest concentration, 10 ppm (curve c), and increase at higher concentrations such as 123 ppm (curve b). However, at the highest concentration of 493 ppm (curve a), while the initial rate of fluorescence increase is greatest, a conspicuous overshoot does not occur.

To probe the extent to which signal from free FPEO chains might obscure the overshoot, Figure 9 compares the adsorption of two FPEO solutions designed to have the same large bulk fluorescence signal. Both runs were conducted at a wall shear rate of 8 s^{-1}. The first solution (curve a) contained 500 ppm FPEO and the

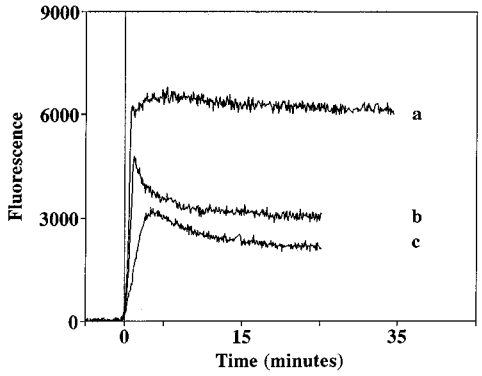

Figure 8. Adsorption of FPEO solutions at a wall shear rate of 13 s^{-1}: (a) 493, (b) 123, and (c) 10 ppm.

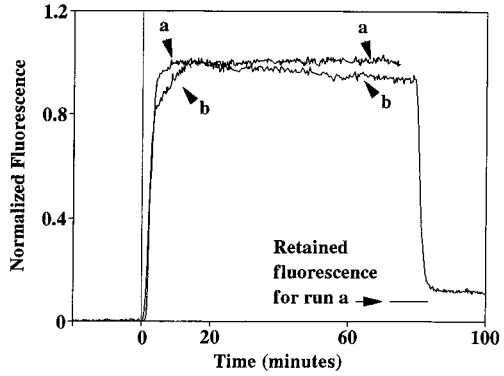

Figure 9. Adsorption at 8 s^{-1} of the following solutions: (a) 500 ppm FPEO; (b) a mixture containing 2 ppm FPEO and free fluorescein. Both solutions have the same bulk fluorescence.

second solution (curve b) contained 2 ppm FPEO and sufficient free fluorescein to achieve the same bulk fluorescence as the 50 ppm solution. Previous experiments established that free fluorescein did not adsorb on silica.[17,19,22] Thus, the clear differences between the two adsorption curves reflect real differences in adsorption behavior of the two concentrations of polymer: Curve b, the 2 ppm FPEO solution doped with fluorescein, displays a large, rapid initial fluorescence increase followed by a slowly increasing kink. The first rise is attributed to the diffusion of free fluorescein from the bulk solution into the evanescent zone, cell filling, and scattering effects that occur on a time scale comparable to filling the cell. The subsequent gradual rise results from adsorption of FPEO on the silica surface and a mild maximum is apparent at 15 min. Upon flushing the cell with PBS, there is a rapid drop in fluorescence, with a magnitude similar to that of the initial fluorescence rise. This drop also occurs on a time scale comparable to the residence time of the cell. The retained coverage is similar to the net signal increase from the time of the kink to the end of the contact period. For curve a, the 500 ppm FPEO solution, there is also a large, rapid, initial fluorescence rise that plateaus relatively quickly. No conspicuous overshoot or kinks are evident. This suggests that the adsorption is over by the time the cell is filled, due to an intrinsically different adsorption process.

4. Measurement of the Diffusion Coefficient. Use of the Leveque approximation in eq 6 to estimate the transport-limited adsorption rate requires independent knowledge of the free solution diffusion coefficient of the adsorbing species: presumably single FPEO chains. Since our FPEO sample was polydisperse, and since the TIRF method is sensitive to interfacial chain *number*, we attempted to directly measure an average

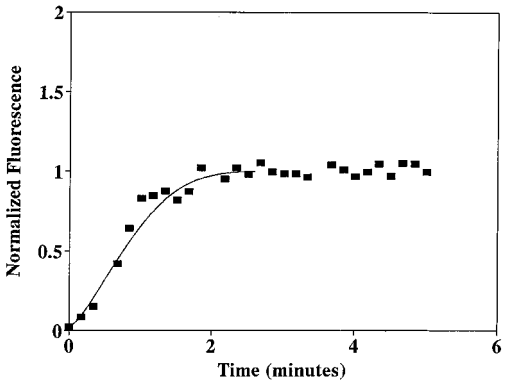

Figure 10. Comparison of signal rise of 20 ppm nonadsorbing FPEO solution flowing over a preadsorbed FPEO layer to best fit of convection diffusion model to determine free species diffusivity.

Table 1. Effect of Bulk Polymer Concentration on TIRF-Measured Diffusion Coefficient and Coil Radius

bulk polymer concn (ppm)	diffusion coeff (cm^2/s)	hydrodynamic coil radius (nm)
20	$(3.1-5.7) \times 10^{-7}$	3.8−7.0
100	4×10^{-8}	55
200	4×10^{-8}	55
6255	4×10^{-8}	55

diffusion coefficient for our sample rather than relying exclusively on published diffusivity data for PEO. This exercise also provided insight into the nature of the adsorbing species and the impact of FPEO concentration on the adsorption mechanism.

Experiments targeting the bulk diffusion coefficient followed the procedure of Santore *et al.*[28] An FPEO layer was preadsorbed onto the silica surface from an FPEO solution at the concentration of interest. After the adsorption process was complete, as gauged by a level TIRF signal, flowing PBS was introduced into the channel to reveal the fluorescence signal due exclusively to the adsorbed layer. This fluorescence level was then treated as background in the diffusion study to follow. The original FPEO solution was reintroduced and the signal recorded as free chains diffused into the evanescent zone and fluoresced. In these experiments, no adsorption took place during the reintroduction of the FPEO solution because the surface was already saturated. Hence the time evolution of the signal was dominated by the free solution diffusivity of the FPEO toward the surface. Results for the signal evolution were compared with the solution of eq 1 (which was convoluted with an exponential decay of the evanescent wave[27]) with the boundary conditions from eqs 4 and 5. An example of this comparison for an FPEO solution at a concentration of 20 ppm and flowing at a wall shear rate of 8 s^{-1} is shown in Figure 10. Here the fluorescence change upon FPEO reintroduction is normalized from 0 to 1 with the fluorescence of the preadsorbed layer included in the zero signal level. The line for $Pe = 1290$ gave the best fit and enabled conversion of the dimensionless time to real time on the abscissa. The experimentally measured diffusivity of $D = 4 \times 10^{-7}$ cm^2/s compares well within the range reported for single PEO chains of molecular weight 18−145K.[29]

Measurements of the diffusion coefficients for several concentrations of FPEO are summarized in Table 1. The error margin in the table represents the precision of the fit comparing the numerical and experimental data for a single experiment. The precision was found by fitting several curves that differed in *Pe* to the data, identifying an acceptable range of fits, and calculating the diffusion

coefficients based on that range. The reproducibility of these diffusivity measurements was generally well within the precision, except as noted. The Stokes–Einstein equation was employed to calculate a hydrodynamic radius of the diffusing species. The values, which ranged from 3.8 to 55 nm, are also given in Table 1. The data obtained at high FPEO concentration reveal slower diffusive processes indicative of a larger diffusing species, presumably PEO clusters. The reduction in diffusion coefficient may be considered conservative since the increased background at high FPEO concentrations tends to artificially decrease the apparent time of signal rise in a diffusion experiment.

The high-concentration data in Table 1 were obtained with solutions that were 6 weeks old. Further tests with 200 ppm solutions revealed that the age of the solution (following dilution from the stock) appeared to influence the nature of the diffusing species. For example, a single chain species was indicated in more than half of the runs conducted with 200 ppm FPEO solutions tested within a week after preparation.

Discussion

The overshoot during the adsorption of FPEO on silica has been shown to be the dominating feature of the surface signal, especially for adsorption from extremely dilute solutions. Establishing the direct cause of the fluorescence decay produced by chains in the adsorbed layer is prerequisite to interpreting the body of data presented here in the context of physical processes that occur during adsorption. Before beginning, however, it is important to address issues concerning the linearity of the TIRF signal in interfacial fluorophore number.

1. Signal Linearity. Experimental evidence points toward a proportionality between the TIRF signal and the interfacial fluorophore number (signal linearity) in the early stages of adsorption, up to the point of the signal maximum. Previous experimental studies suggest that PEO adsorption on silica is transport limited, at least up to 80% of full coverage.[5,6] We agree qualitatively with the literature, in that Figure 6 demonstrates a significant influence of the wall shear rate on the adsorption rate, per eq 6. (A quantitative kinetic analysis of the initial stages of the TIRF-measured FPEO adsorption, not restricted to the assumptions of the Leveque treatment, is presented elsewhere.[30]) Our findings are also consistent with the notion of transport-limited adsorption because at dilute solution conditions where single chains dominate the diffusion coefficient, we observed a proportionality between the bulk concentration and the initial rise of the signal during adsorption runs. The fact that we consistently observe nearly linear signal rises (with respect to time) and a concentration dependence of the initial slope supports TIRF signal linearity in this early phase of adsorption.

The TIRF signal linearity persists over the majority of the period in which surface mass accumulates, as is shown in Figure 11, which provides an approximation of the surface coverage associated with the maximum. In Figure 11, for an adsorption run with a concentration of 2 ppm and a wall shear rate of 8 s^{-1}, the time axis is converted to a surface coverage, employing the Leveque approximation for adsorption rate in eq 6 and using the independently measured single-chain diffusivity (4×10^{-7} cm^2/s) in Table 1. This mass accumulation scale applies only to the linear portion of the signal rise and, at the maximum of this particular experiment, a coverage of 0.7 mg/m^2 is calculated. (Surface coverages near

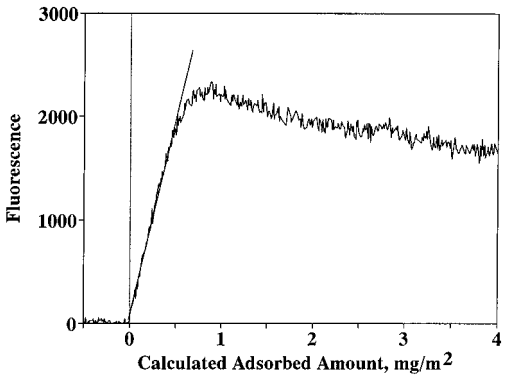

Figure 11. Calculated adsorbed amount of FPEO vs fluorescence using the Leveque approximation. The data were obtained at a wall shear rate of 8 s^{-1} and an FPEO solution concentration of 2 ppm.

1 mg/m^2 are typically found for this molecular weight range of PEO on silica,[5,6] leading to the conclusion of TIRF signal linearity up to the time of the maximum and that the surface is nearly saturated at the maximum.) The surface coverages calculated for FPEO adsorption from dilute solution (single-chain diffusion) by this method were always between 0.7 and 0.8 mg/m^2 at the maximum, for solutions containing only FPEO, as opposed to mixtures with unlabeled chains. An interpretation of the timing of the maxima in mixtures is presented later.

At long times, well beyond the maximum, the signal was also nearly linear in interfacial fluorophore number, as the ultimate fluorescence levels were consistent with general expectations and those based on the silica particle isotherms in Figure 1. For example, in Figure 3 when unlabeled chains were introduced mid-run, the fluorescence signal ultimately fell below that for the uninterrupted run where fluorophore-containing chains had continuous access to the surface. At long times, the experiments with unlabeled PEO should eventually approach zero fluorescence as unlabeled chains replace the original FPEO chains on the surface, and the uninterrupted FPEO runs should approach finite fluorescence levels. Both limiting cases were approached in Figure 3, albeit rather slowly. The qualitative consistency between Figure 1 and the ultimate signal levels in Figure 4 also argues in favor of long-time signal linearity in interfacial fluorophore number. Figure 1 suggests that high molecular weight (unlabeled) chains should adsorb preferentially from mixtures, and TIRF exhibits a low ultimate signal for the mixture containing 400K unlabeled chains in Figure 4. For the mixture containing 20K chains, the ultimate signal level in Figure 4 was similar to that for the control run. This observation agrees with the conclusion from Figure 1 that labeled FPEO chains and unlabeled 20K chains are in close competition at low converages but that the higher molecular weight labeled FPEO chains ultimately dominate the surface.

While observations favor a proportionality between the TIRF signal and interfacial fluorophore number in the early and late stages of the experiments, the most interesting kinetics near the overshoot may result from signal linearity near the time of the overshoot combined with a maximum in the interfacial fluorophore number, or there may be a temporary breakdown of the signal linearity through quantum yield changes. Near the maximum, the issue of signal linearity becomes entangled with polymer physics issues, since chain reconfigurations might influence the quantum yield.

2. Causes for the Signal Decrease. Two types of phenomena potentially explain the decreasing TIRF signal in the intermediate stages of adsorption. The first is a molecular weight driven exchange (which might occur without changes in the quantum yield), and the second is interfacial chain reconfigurations which significantly decrease the quantum yield of fluorophores on adsorbed chains.

The concept of molecular weight driven exchange is consistent with transport-limited adsorption. Here short chains diffuse rapidly to the surface at short times but are eventually displaced by higher molecular weight chains, slower to diffuse to the surface but ultimately preferred at equilibrium. The exchange process drives the signal down because long chains contain fewer labels per until mass than short chains. The hypothesis of molecular weight driven exchange provides an interpretation of Figure 3 where exchange is prevented by removal of free chains from the chamber (PBS introduction) and where the signal drops more rapidly upon the introduction of unlabeled high molecular weight chains. (The slow decay in curve b of Figure 3 is then attributed to exchange with chains previously adsorbed on the flow lines. This potentially maintains a low concentration of free chains in the cell, even though it is intended that only PBS be present.) Exchange is also supported by the transport-limited adsorption kinetics illustrated in Figure 6. Here, the wall shear rate sensitivity of the decay suggests that exchange, if it occurs, is not rate-controlled by the desorption of preadsorbed chains (at least for the layer maturities and time scales pertinent to this study.) Exchange is also consistent with the double overshoot in Figure 4: Here the initial signal rise is attributed to the domination of the surface by the lower molecular weight populations within the FPEO sample. Then the first maximum and intermediate decay occur when the unlabeled 20K PEO chains displace the shorted labeled chains on the surface. The signal rises again as labeled chains, exceeding 20K in molecular weight, displace the unlabeled 20K chains. The signal ultimately drops when the longest chains adsorb and displace shorter ones.

Another argument favoring molecular weight driven exchange is the realization that it requires removal of only a small mass of short chains to produce a large decrease in the fluorescent signal. A simple calculation reveals a 50% decrease in the expected fluorescence signal for the desorption of a labeled population of chains of 5K molecular weight that comprise 5 mass % of an FPEO layer and where the balance of the chains has 1 label for every 92K molecular weight. In the longest FPEO adsorption run done in the TIRF, 24 h, the fluorescent signal fell to 30% of its maximum value; hence the magnitude of the signal change is qualitatively consistent with the expected sensitivity of TIRF to low molecular weight FPEO populations.

One point worth mentioning is that the molecular weight driven exchange of PEO on silica, studied by Dijt *et al.*[5] using reflectivity, was found to be very rapid: mass transfer limited with local equilibrium between the adsorbed layer and the fluid nearest the surface. Our findings agree with the previous results only to a certain extent. In addition to transport-limited kinetics at short and intermediate times, we find continued decays at long times up to 24 h and, in Figure 3, retention of labeled FPEO on surfaces exposed to higher molecular weight unlabeled PEO. Discrepancies between Dijt's work and ours may result from the greater sensitivity of TIRF (compared with reflectivity) to labeled interfacial populations in a mixture. Also, through quantum yield effects, TIRF may be sensitive to very slow interfacial relaxations, not detectable with reflectivity.

A final observation in favor of molecular weight driven exchange is that overshoots were not observed for the adsorption of randomly fluorescently tagged (hydroxyethyl)cellulose on silica,[17] a system which will yield a TIRF signal proportional to interfacial mass as a result of random labeling. Clearly, the best test of the molecular weight driven exchange hypothesis would be the adsorption of a narrow molecular weight distribution sample of FPEO. This was not available, because of the degradation which occurred as part of the dialysis and storage procedures for FPEO.

A second explanation for the TIRF signal decrease in the intermediate stages of FPEO adsorption is interfacial reconfigurations reducing the quantum yield, most likely through fluorophore−fluorophore interactions or the effect of the local environment. Fluorophore−surface interactions are thought not to be involved with the overshoot, because their probability of occurrence would be highest at low coverages and diminish as the adsorption process continues, causing a signal enhancement rather than a decay. Figures 3 and 6 illustrate that the overshoot is related to the rate of incoming chains, not to processes intrinsic to the surface. Therefore, we also know that any reconfigurations associated with the overshoot are not relaxation driven, i.e. not due to the slow evolution of the surface toward an equilibrium state. Indeed, the wall shear rate sensitivity of the decay suggests that the surface is very local equilibrium. Furthermore, in Figure 3 it is clear that unlabeled chains can produce the decay as well as labeled chains, indicating that the decay is not caused by the enhancement of fluorophore−fluorophore interactions through the addition of more fluorophores to the layer. Therefore, if the overshoot is a result of interfacial chain reconfigurations, it reflects the dependence of the average interfacial chain configuration on surface loading, at local equilibrium between the adsorbed layer and the fluid nearest the surface. Fleer *et al.*[1] present calculations of the coverage dependence of the hydrodynamic layer thickness: The thickness develops dramatically near saturation, predictions confirmed by studies of poly(vinylpyrolidone) on silica and PEO on silica and PS.[1] As saturation is approached, incremental changes in surface mass cause chain ends to protrude from the layer to form hydrodynamically influential tails. It may be that TIRF signal from FPEO is sensitive to tail formation (while randomly tagged HEC is insensitive to the chain ends) through quantum yield effects. These could result from a mobility sensitive or chemical environment influenced quantum yield. For example, the formation of eximers requires fluorophore mobility.

The observation of a double overshoot in Figure 4 is also consistent with the hypothesis that interfacial chain configurations might influence quantum yield, giving the following interpretation of Figure 4: Adsorption proceeds at the mass transport limited rate, with each population of varied molecular weight adsorbing according to the rate controlled by its diffusion coefficient. We know that low molecular weight homopolymers have slightly lower equilibrium coverages (approach saturation sooner) than longer chains of the same chemistry.[1] We also know that as surfaces saturate, chain ends extend into solution.[1] In a mixture containing polydisperse FPEO and a population of 20K chains of narrow molecular weight distribution, the initial signal rise corresponds to the arrival of different molecular weight

populations, with the surface dominated by smaller chains. At intermediate times, the surface is dominated by the unlabeled 20K population. At this point, the surface no longer accepts the shortest chains in the solution. Further adsorption of populations that are 20K or longer causes a net signal decrease because the quantum yield of the labels on short chains decreases as the short chains reconfigure. The signal rises again during the time where the surface reaches its maximum coverage of unlabeled 20K chains: their reconfiguration is not visible. Finally, when the surface saturates with the highest molecular weight populations, the longest tails extend into solution, causing a reduction in interfacial fluorescence. This quenching mechanism for signal reduction does not exclude the possibility that short chains are replaced by long ones, also contributing to a decrease in signal. The important observation is that either process for interfacial signal reduction, molecular weight driven exchange or interfacial reconfigurations, is a sequential dynamic process on the surface which is dominated by different molecular weight populations: short chains at short times and long chains at long times.

3. Concentration Effects. For dilute polymer solutions, single-chain diffusion was found to dominate the adsorption process. The proportionality between the initial slope and bulk concentration and between the initial decay rate and the bulk concentration supported transport-limited adsorption. At concentrations exceeding 100 ppm, diffusion to the surface was sometimes (depending on the solution age) dominated by polymer clusters. Also, the overshoots were observed to be intermittent and less pronounced at higher concentrations, rarely occurring for bulk concentrations near 500 ppm.

Several factors may contribute to the disappearance of the overshoot at high concentrations. First, clusters delivering groups of chains of varied molecular weight all at once to the surface disrupt the molecular weight sequence of populations which dominate surface. Also, even without clusters, at high concentrations, the chain arrival rate may exceed the rate of chain attachment, causing adsorption to no longer be transport limited. Finally, with rapid adsorption from solution, early arriving chains may not have time to spread on the surface, so when the surface does saturate, the extent of chain reconfiguration is less severe than what may occur at low concentrations. That is, if the surface saturates quickly with all the chains adsorbing at once, tails might always be present. Indeed, the signal levels from layers adsorbed from concentrated (500 ppm) solutions were similar to the ultimate levels achieved for adsorption from dilute solutions, after 24 h of equilibration.

4. Events Controlling the Timing of the Maximum. The duration of the linear signal rise can provide additional insight into the physics of adsorption. In this discussion, we are interested in the timing of what we call the primary maximum, which occurs spontaneously when all chains each bear a single label, as in the control FPEO studies like that in Figure 11. This is contrasted with the first maximum in curve b of Figure 4, which results from the unlabeled population of 20K molecular PEO. If the signal is linear in interfacial fluorophore number, the primary maximum occurs when the number flux of chains at the interface vanishes. Prior to the maximum, the number of chains on the surface increases dramatically and after the maximum the interfacial chain number is reduced. Figure 11 and reflectivity results in our laboratory[7] indicate that the maximum occurs at a time when the surface is nearly saturated. Processes after the maximum are still controlled, however, by the rate of chain arrival from bulk solution. Of particular interest is whether the filling of the surface (by all species) is the primary event which triggers the sharp turnover in the signal, and the extent to which the relative adsorbed amounts of high and low molecular weight species influence the timing of the overshoot.

Table 2. Effect of Composition and Wall Shear Rate of Time to Maximum Fluorescence and Calculated Adsorbed Amount

soln comp (2 ppm total polymer)	time to max fluorescence (min)
FPEO, 0.8 s^{-1}	59
50/50 FPEO/unlabeled 20K PEO, 0.8 s^{-1}	25, 125
50/50 FPEO/unlabeled 100K PEO, 0.8 s^{-1}	22.5
50/50 FPEO/unlabeled 400K PEO, 0.8 s^{-1}	30
FPEO, 8 s^{-1}	20
FPEO, 80 s^{-1}	8.4

Through the primary overshoot occurs near the time of surface saturation, we feel it is not the overall "filling" of the surface which triggers the signal decay. TIRF is sensitive to low molecular weight populations which, according to mean field theories,[1] will have lower coverages on the plateaus of their adsorption isotherms than higher molecular weight samples. Though our sample is somewhat polydisperse, the molecular weight ratio of the longest and shortest chains (where both populations must be sufficiently large to contribution to the surface mass) is probably about 4−7, because our sample was originally a 97K narrow molecular weight standard which degraded. (The GPC results are not sufficiently precise to resolve the ratio exactly.) Therefore in our sample, the plateau coverage of the lower molecular weight cut (which must be defined to include a significant mass fraction of the sample) may be slightly less than that of the longest chains. This suggests that the maximum fluorescence occurs when the short chains reach local equilibrium. This would diminish their flux, although long chains would continue to add to the surface.

The time to achieve the maximum fluorescence, summarized in Table 2 for several studies, with the values representing averages of several runs, is found to correlate with the amount of high molecular weight chains in the bulk solution. For adsorption from 2 ppm FPEO at a wall shear rate of 0.8 s^{-1}, the maximum occurs approximately 1 h into the run. This control FPEO solution contains some high molecular weight species which eventually dominate the surface; however, we do not know their concentration in the bulk solution.

For the two mixtures containing unlabeled long chains (100K or 400K molecular weight) mixed 50−50 with FPEO to achieve a solution with an overall concentration of 2 ppm, the time to the maximum fluorescence was approximately half that of the control runs. These mixtures contained half of the labeled long chains from the control FPEO solution, plus a full ppm of unlabeled long chains. Therefore the total amount of high molecular weight species was increased by ∼1 ppm over that in the control sample. These mixtures also contained half the low molecular weight species of the control FPEO sample. If the short-chain concentration were the only feature controlling the timing of the maximum, one would expect that the time of the maximum for these mixtures would be twice that seen in the control run. The observation of a reduced time for the fluorescence maximum suggests that the unlabeled long chains occupy a significant portion of the

surface, such that the labeled short chain flux to the surface vanishes earlier in the run.

The results from the mixture of labeled FPEO with 50 mass % unlabeled 20K chains are consistent with the idea of competitive adsorption and local equilibria. When the mixture is richer in low molecular weight species (a significant number of which are unlabeled and 20K in molecular weight), the primary maximum occurs at 125 min, approximately twice that of the control experiment. Because the concentration of low molecular weight chains is greater in this sample, it would be expected that the surface would equilibrate locally with the low molecular weight chains in a shorter time when the control study with pure FPEO. Observations indicate the opposite: The increased time to maximum must therefore result from the reduced labeled long chain concentration: a greater amount of time is needed before the surface is nearly saturated with the long chains.

Conclusions

This work explored several facets of PEO adsorption and the use of TIRF to study adsorption kinetics. Kinetic arguments were presented for a proportionality between the TIRF signal and number of interfacial fluorophores in the early stages of adsorption. A proportionality between TIRF signal and the number of interfacial fluorophores at long times was supported by comparison of TIRF data to isotherms involving polymer mixtures. The most interesting feature of PEO adsorption was an overshoot at intermediate times.

The work revealed several fundamental features of PEO adsorption onto silica. A wall shear rate sensitivity of the adsorption rate and a proportionality between the adsorption rate and the solution concentration (in dilute solutions) suggested transport-limited adsorption kinetics up to coverages of 0.7 mg/m^2. It was found that for solutions more dilute than 50 ppm, single chains diffused to the surface while at higher concentrations, clusters dominated the diffusion step and potentially changed the physics of adsorption. This work also demonstrated a method by which free solution diffusivities can be measured with TIRF.

The overshoot occurring in the intermediate stages of PEO adsorption was shown to be highly sensitive to the molecular weight distribution in the adsorbate solution, with the potential to resolve populations of different molecular weights within a single sample. The decay process associated with the overshoot was attributed to one or both of the following sequential dynamic mechanisms: (1) replacement of initially adsorbed short chains by longer chains preferred on the surface at equilibrium and (2) reconfiguration of adsorbed chains altering the mobility and chemical environment surrounding the fluorescent tag on the chain end. Either explanation is consistent with the observation that the rate of signal decay after the maximum was dependent on the rate of new chain arrival to the surface.

Acknowledgment. This work was made possible by the support from the Petroleum Research Foundation (23917-G7), the National Science Foundation (CTS 9209290), the Dana Foundation, and Lehigh's Chemical Engineering Department and Polymer Interfaces Center. Special thanks go to S. T. Milner for helpful discussions.

References and Notes

(1) Fleer, G. J.; Cohen Stuart, M. A.; Scheutjens, J. M. H. M.; Cosgrove, T.; Vincent, B. *Polymers at Interfaces*; Chapman and Hall: London, 1993.
(2) Kawaguchi, M.; Hayakawa, K.; Takahashi, A. *Macromolecules* **1983**, *16*, 631−635.
(3) Lee, J. L.; Fuller, G. G. *J. Colloid Interface Sci.* **1985**, *103*, 569−577.
(4) Malmsten, M.; Linse, P.; Cosgrove, T. *Macromolecules* **1992**, *25*, 2474.
(5) Dijt, J. C.; Cohen Stuart, M. A.; Fleer, G. J. *Macromolecules* **1994**, *27*, 3219−3228.
(6) Dijt, J. C.; Cohen Stuart, M. A.; Hoffman, J. E.; Fleer, G. J. *Colloids Surf.* **1990**, *51*, 141−158.
(7) Fu, Z.; Santore, M. M. Manuscript in preparation.
(8) Pefferkorn, E.; Carroy, A.; Varoqui, R. *J. Polym. Sci., Polym. Phys. Ed.* **1985**, *23*, 1997−2008.
(9) Pefferkorn, E.; Carroy, A.; Varoqui, R. *Macromolecules* **1985**, *18*, 2252−2258.
(10) Leermakers, F. A.; Gast, A. *Macromolecules* **1991**, *24*, 718−730.
(11) Parsons, D.; Harrop, R.; Mahers, W. G. *Colloids Surf.* **1992**, *64*, 151−160.
(12) Dorgan, J. R.; Stamm, M.; Toprakcioglu, C.; Jerome, R.; Fetters, L. J. *Macromolecules* **1993**, *26*, 5321−5330.
(13) Tilton, R. D.; Robertson, C. R.; Gast, A. P. *Langmuir* **1991**, *7*, 2710−2718.
(14) Johnson, H. E.; Clarson, S. J.; Granick, S. *Polymer* **1993**, *34*, 1960−1962.
(15) Rebar, V. A.; Santore, M. M. *Prog. Rep. Lehigh Univ. Polym. Interface Center*, **1992**, *1*, 29−40.
(16) Santore, M. M.; Rebar, V. A. In *Dynamics in Small Confining Systems II*; Drake, M., Troiian, S. M., Klafter, J., Kopelman, R., Eds., MRS Symp. Ser. 366; Materials Research Society: Pittsburgh, 1995.
(17) Rebar, V. A.; Santore, M. M., first paper in this series (this issue).
(18) Kelly, M. S.; Santore, M. M. *J. Appl. Polym. Sci.* **1995**, *58*, 247−263.
(19) Kelly, M. S.; Santore, M. M. *Colloids Surf. A: Physiochem. Eng. Aspects* **1995**, *96*, 199−215.
(20) Rebar, V. A. Ph.D. Dissertation, Lehigh University, 1995.
(21) Rebar, V. A.; Santore, M. M. *J. Colloid Interface Sci.* **1996**, *178*, 29−41.
(22) Slavik, J. *Fluorescent Probes in Cellular and Molecular Biology*; CRC Press Inc.: Boca Raton, FL, 1994.
(23) Darst, S. A.; Robertson, C. R.; Berzofsky, J. A. *J. Colloid Interface Sci.* **1986**, *111*, 466−474.
(24) Lok, B. K.; Cheng, Y. L.; Robertson, C. R. *J. Colloid Interface Sci.* **1983**, *91*, 104−116.
(25) Shibata, C. T.; Lenhoff, A. M. *J. Colloid Interface Sci.* **1992**, *148*, 485−507.
(26) Leveque, J. *Ann. Mines* **1928**, *13*, 284.
(27) Kelly, M. S. Master's Thesis, Lehigh University, 1993.
(28) Santore, M. M.; Kelly, M. S.; Mubarykan, E.; Rebar, V. A. In *Surfactant Adsorption and Surface Solubilization*; ACS Symp. Ser. 615; Sharma, R., Ed.; American Chemical Society: Washington, DC, 1995; pp 183−195.
(29) Sauer, B. B.; Yu, H. *Macromolecules* **1989**, *22*, 786.
(30) Santore, M. M.; Rebar, V. A.; Kelly, M. S., submitted to *Colloids Surf. A.*

MA951237W